RSC Advances

ROYAL SOCIETY OF CHEMISTRY

www.rsc.org/advances

1 Preparation of cellulose-graft-polylactic acid via melt copolycondensation for use in

2 polylactic acid based composites: synthesis, characterization and properties

3

4 Sun Hua, Feng Chen, Zheng-ying Liu, Wei Yang, Ming-bo Yang*

5 College of Polymer Science and Engineering, State Key Laboratory of Polymer Materials Engineering,

6 Sichuan University, Chengdu 610065, Sichuan, People's Republic of China

7

8 **Abstract**: In order to improve the melt strength of poly(lactic acid) (PLA), microcrystalline

9 cellulose-graft-polylactic acid (MCC-g-PLA) copolymer was prepared and introduced into PLA

10 matrix. The MCC-g-PLA copolymers were synthesized by melt copolycondensation of lactic acid

11 (LA) with microcrystalline cellulose (MCC) which was pretreated to improve accessibility. The

12 MCC-g-PLA copolymers with a molar substitution (MS) of PLA in range of 1.67-5.97 were

13 synthesized by adjusting reaction temperature, molar ratio of LA monomer to MCC and washing

14 times in pretreatment process. Compared with MCC, the crystalline structures of MCC-g-PLA

15 copolymers were not perfect due to the existence of PLA side chains. A glass transition

16 temperature (T_g) appeared in the copolymers, which had never been observed in unmodified MCC,

17 and decreased with the increase of MS. When MS was above 4.41, the thermal degradation of

18 PLA side chains emerged. When MCC-g-PLA copolymer was introduced into PLA matrix, well

19 dispersion of MCC-g-PLA was verified with SEM results. The extension rheology results showed

20 that the melt strength of PLA can be effectively enhanced with the addition of MCC-g-PLA,

21 especially at low elongation rate. Meanwhile, MCC-g-PLA also improved the crystallization

22 ability of PLA in non-isothermal crystallization process.

23

24 **Keywords**: Microcrystalline cellulose; Lactic acid; Melt copolycondensation; Graft copolymer;

25 Extensional rheological

26

27 **1. Introduction**

28

29 Poly(lactic acid) (PLA), which holds the potential to replace traditional petroleum based polymer

30 materials because of its excellent mechanical properties, outstanding processing performance,

31 availability from renewable agricultural products and biodegradability, has gained enormous

32 attention [1-3]. It has been widely used in academic researches and industrial applications [4-7], for

33 example stretch-blown bottles [8], scaffold materials [9-11] and so on. Except for these applications, it

34 is noteworthy that PLA should be used as plastic bags and plastic film due to the biodegradability

35 taking the environment problems into consideration [12]. Taking agricultural plastic film as an

36 example, the residue of agricultural plastic film in the field has already become an important

37 negative factor that affects agricultural environment, which destroys the soil structure and harms

38 growth of crop, due to the non-degradable plastic film [13]. So it is of great value to use PLA film

39 instead of traditional plastic film for environment and demanding markets [12].

40 Although PLA possesses many advantages, the drawbacks of the poor viscoelastic behavior, low

41 melt strength, the inherent brittleness, and slow crystallization rate, have limited its large-scale

42 commercialization especially as film materials [14-16]. As is known, blow molding, by which a

43 bi-axial stress is imposed on the film bubble, is the most convenient and

44 high-performance-price-ratio method to manufacture films. From such a process, impact

1 properties of the film are excellent and mechanical and optical properties can be controlled [17].
2 However, polymer melt undergoes a complex three-dimensional deformation process during blow
3 molding, so to prepare blown film steadily and successfully, high melt strength is the basic
4 requirement for materials, such as the case for branched low density polyethylene (LDPE).
5 Unfortunately, the blow molding of PLA is quite difficult owing to its poor viscoelastic behavior
6 and low melt strength. The brittleness of PLA also prevents it from being used as plastic bags and
7 plastic film. Therefore, in order to improve the processability of PLA to be used as blown films
8 and to prepare PLA films with good properties, PLA needs to be modified to improve the melt
9 strength, viscoelastic behavior and toughness [16, 18].
10 Increasing the molecular weight and introducing long branched chains have been proved to be
11 effective methods to improve the melt strength of PLA, which can increase chain entanglement
12 and extend melt relaxation time of PLA chains. Although high molecular weight (Mw) PLA can be
13 synthesized by ring-opening polymerization of lactide and chain extension in laboratory studies [19,
14 20], Mw of commercial PLA is still not high enough to ensure the melt strength needed for blow
15 molding. Introducing the long branched chains is another effective method, which also has a great
16 influence on the viscoelastic behavior of polymer melt, and has been proved to be able to increase
17 the melt strength and chain entanglement [21-23]. So, if we can synthesized copolymer with long
18 branched chains of PLA, the existence of PLA branched chains can not only increase
19 entanglement of PLA chains and melt strength of PLA , but also improve the dispersion state of
20 the copolymer in PLA, thus making PLA easy to process.
21 Cellulose is the most abundant, biodegradable, and renewable natural polymer in the earth, and
22 holds many attractive properties, such as low cost, nontoxic, good mechanical properties and low
23 density [24, 25]. If we can graft long branched chains of PLA onto cellulose, the biodegradable
24 property of products is guaranteed, simultaneously, the applications of PLA and cellulose are both
25 widened.
26 Graft copolymerization is a common way to introduce other polymers onto cellulose or cellulose
27 derivatives [26-32]. Unfortunately, cellulose has strong intramolecular and intermolecular
28 hydrogen-bonding network and high crystallinity, which make it non-thermoplastic and insoluble
29 in common solvent. Most reaction reagents penetrate only into the amorphous regions of cellulose
30 [33], while a lot of hydroxyl groups are sealed in crystalline region, then it is difficult to access to
31 reagents and participate in reaction. These restrict the reaction activity of cellulose. In recent years,
32 new solvents of cellulose have been discovered, such as lithium chloride/N,N-dimethylacetamide
33 and ionic liquid [34-36]. They had been used as reaction media to graft polymer chains onto cellulose
34 [37-42], which could improve the accessibility and reactivity of cellulose. But the use of solvents
35 could bring some problems, such as toxicity, complicated preparation process, or degradability.
36 How can we improve the accessibility of cellulose in non-toxic solvent ? According to previous
37 studies [43-46], treating cellulose with aqueous sodium hydroxide (NaOH) solutions had a
38 considerable effect on the hydrogen-bonding network and crystalline structure of cellulose, in this
39 case the crystalline structure of cellulose can transform from cellulose I to cellulose II. In this
40 process, the alkali can destroy the hydrogen bonds and infiltrate into the crystalline region, which
41 could be utilized to improve the accessibility and activity of cellulose. Then the solvent can be
42 exchanged. Thus, the reaction monomer could get inside of cellulose.
43 Because lactide is easy to decompose, lactic acid was chosen as reaction monomer. In this work,
44 firstly we improved the accessibility of cellulose by solvent exchanged method. Then, melt

copolycondensation of lactic acid with microcrystalline cellulose (MCC) was carried out to obtain microcrystalline cellulose-graft-polylactic acid copolymers using Tin(II) chloride dehydrate catalyst. Finally, the synthesized copolymer was added into PLA matrix, and the properties of PLA composites were studied.

2. Experimental

2.1. Materials

Microcrystalline cellulose (MCC) with a degree of polymerization (DP) of ca. 200 was purchased from ChengDu KeLong Chemical Co., Ltd. China. Lactic acid (chemical grade, solute concentration: 85wt%), sodium hydroxide (NaOH), Tin(II) chloride dihydrate (SnCl$_2$), toluene, dichloromethane, dimethyl sulfoxide (DMSO) and alcohol were reagent grade and purchased from ChengDu HaiHong Chemical Co., Ltd. China. PLA (trade name REVODE110) with a number-average molecular weight of 4×10^4 g·mol^{-1} was purchased from Zhejiang Hisun Biomaterials Co., Ltd. China.

2.2. Introduction of lactic acid to the inside of microcrystalline cellulose

A dissolving procedure of MCC in alkaline solution was performed as follows [47]. 2.5g NaOH was dissolved in 26.9g water at room temperature. 1g MCC was then added into the mixture, resulting in a suspension of MCC in an 8.5wt% NaOH solution. The suspension was put into refrigerator until it became a frozen solid state. The frozen solid was then put into room temperature to thaw, and 20.6g water was added to the thawed mixture with gentle stirring, and a clean solution was obtained. The dissolved cellulose was precipitated with lactic acid and filtrated, and then the precipitate was washed with LA for 4 times, dried in an oven at 60 ^{o}C, and was coded as MCC-L. The weight of MCC-L was 26.2g.

As a contrast, using the same process, we used water to precipitate the dissolved cellulose and wash the precipitate, then the product was dried in an oven at 60 ^{o}C, and was coded as MCC-W. The weight of MCC-W was 0.9g.

2.3. Synthesis of MCC-g-PLA copolymers

The undried MCC-L and lactic acid monomer (molar ratio of LA/AHG was 36/1) were put into a three-neck flask equipped with a mechanical stirrer and a thermometer. The system was heated in an oil bath and dehydrated under vacuum condition at 100 ^{o}C, 110 ^{o}C and 120 ^{o}C for 2h, respectively. After dehydration, the temperature was heat up to initial reaction temperature, and then catalyst SnCl$_2$ was added into flask. Then the absolute pressure was reduced to 500-700Pa, and the melt copolycondensation was carried out by heating the reaction system at a gradient style to prevent the evaporation of LA molecules in early stage (specific reaction temperature and time was in the order as follows: 130 ^{o}C, 2h; 140 ^{o}C, 2h; 150 ^{o}C, 2h; 160 ^{o}C, 2h). After the reaction finished, 200ml dichloromethane was poured into the flask. The resultant polymer was precipitated with alcohol, and then was extracted with toluene in a Soxhlet extraction apparatus for 24h to remove the byproduct (homo-PLLA) formed in reaction. The purified product was soaked with dichloromethane for hours, and was filtered until the filtrate became transparent and

1   no precipitate appeared when a few drops of filtrate were put into alcohol, which could confirm
2   that no byproduct remained and the purification was sufficient. Finally the product, MCC-g-PLA,
3   was dried in an oven at 60 $^\circ$C for over 24h, and was coded as MP-C2W4-T160, in which C
4   represented the content of LA, W represented the washing times with LA in pretreatment, and T
5   represented the maximum reaction temperature. Using the same process and adjusting reaction
6   conditions or molar ratios of LA monomer to anhydroglucose (AHG) , a series of MCC-g-PLA
7   copolymers were prepared. The reaction conditions, molar ratios of LA monomer to MCC and
8   reaction results were summarized in Table 1.
9
10   **2.4 Preparation of PLA/MCC-g-PLA composites**
11
12   Composites of PLA with MCC-g-PLA were prepared by solution mixing. PLA and MCC-g-PLA
13   (sample MP-C2W1-T160 was used) were dissolved separately in DMSO before mixing. The
14   concentrations of PLA/DMSO and MCC-g-PLA/DMSO were 3g/100ml and 3g/1000ml
15   respectively. The two solutions were then mixed and the mixture was ultrasonically treated for
16   30min. Subsequently, the mixture was precipitated in alcohol and dried to a constant weight at 60
17   $^\circ$C in a vacuum oven, and finally the composites PLA/MCC-g-PLA were obtained. The
18   composites were coded as PLA-MP-X, in which X represented the weight of MCC-g-PLA in 100g
19   PLA matrix and X was 2, 3, and 4, respectively. As a contrast, composites of PLA with
20   unmodified MCC were prepared using the same process, and were coded as PLA-MCC-X, in
21   which X represented the weight of MCC in 100g PLA matrix, and X was 2, 3, and 4, respectively.
22
23   **2.5. Characterization**
24
25   2.5.1. Fourier transforms infrared (FTIR) spectrometry
26   The molecular structure of MCC-g-PLA by melt copolycondensation was confirmed by Fourier
27   Transform Infrared Spectroscopy (FTIR) using a Nicolet 6700 FTIR spectrometer (Nicolet
28   Instrument Company, USA) at the wavelength range of 650-4000 cm^{-1} with a resolution of 4 cm^{-1}
29   in the transmission mode. Samples of MCC and MCC-g-PLA copolymers were respectively
30   mixed with KBr powders and pressed into a disk for FTIR measurement.
31
32   2.5.2. ^{1}H nuclear magnetic resonance (^{1}H NMR)
33   The contents of grafted PLA in MCC-g-PLA copolymers were characterized by ^{1}H nuclear
34   magnetic resonance (NMR) spectroscopy. ^{1}H NMR spectra were recorded on a Bruker AV II-600
35   MHz spectrometer (Bruker Company, Switzerland) in dimethyl sulfoxide-d_6 (DMSO-d_6) solvent
36   with tetramethysilane (TMS) as an internal standard. A drop of trifluoroacetic acid-d was added
37   into the DMSO-d_6 to shift active hydrogen to lower field area, in order to reduce the influence of
38   active hydroxyl and water on the subsequent calculation. Other measuring conditions were as
39   follows: solute concentration, 6mg/ml; temperature: ambient temperature.
40
41   2.5.3. Wide-angle X-ray diffraction (WAXD)
42   The crystalline structures of MCC, MCC-L, MCC-W and MCC-g-PLA copolymers were studied
43   by WAXD. WAXD patterns of the samples were obtained with a DX-1000 diffractometer
44   (Dandong Fangyuan Instrument Company, China) with Cu Ka radiation (wave length=0.154 nm)

1   under 40 kV and 25 mA at ambient temperature. Samples were scanned over the range of

2   diffraction angle 2θ=5~40° with a scan speed of 3 °/min at room temperature.

3

4   2.5.4. Differential scanning calorimetry (DSC)

5   To get the glass transition temperature (T_g) of MCC-g-PLA copolymers, differential scanning

6   calorimetry (DSC) analysis was implemented on a TA Instrument DSC Q20 (TA Instruments Inc.,

7   USA) under nitrogen atmosphere. Before measurement, the samples of 5~7mg were dried at 60 °C

8   for 24h, and then were heated from -25 °C to 180 °C and kept at 180 °C for 5 min to eliminate the

9   thermal history. Finally they were cooled to -25 °C and reheated to 180 °C. The scanning rate was

10   10 °C/min. The second heating curves were recorded to determine the T_g of samples.

11   The thermal analysis of PLA/MCC-g-PLA composites was also performed by DSC. The samples

12   of 5~7mg were dried at 60 °C for 24h before measurement, and were heated from 25 °C to 200 °C

13   at a heating rate of 10°C/min and kept at 200 °C for 3min to eliminate the thermal history, then

14   cooled to 25 °C at a rate of 5 °C/min, and finally were reheated to 200 °C at a rate of 10 °C/min

15   under nitrogen atmosphere. The cooling and second heating curves were recorded.

16

17   2.5.5. Thermogravimetric analysis (TGA)

18   To characterize the thermal stability of MCC-g-PLA copolymers, thermogravimetric analysis

19   (TGA) was performed on a thermogravimetric analyzer (TGA Q600, TA Instruments, USA) from

20   30 to 800 °C at a heating rate of 10 °C/min under nitrogen atmosphere.

21

22   2.5.6 Scanning electron microscope (SEM)

23   The dispersion of MCC-g-PLA in PLA matrix was examined using a scanning electron

24   microscopic (SEM) (JEOL JSM-5900LV, JEOL PTE Ltd., Tokyo, Japan) at an accelerating voltage

25   of 5kV. The samples for SEM observation were compression molded into 0.1mm thickness at 180

26   °C and 10 MPa, and then were fractured manually after immersion in liquid nitrogen for 1h.

27   Before observation the fracture surfaces were coated with a thin layer of gold.

28

29   2.5.7. Extensional rheology

30   Uniaxial extensional rheological behavior of PLA/MCC-g-PLA composites was conducted on an

31   ARES extensional rheometer with the extensional viscosity fixture (EVF, TA Instruments, USA) at

32   158.5 °C at extensional strain rates of $0.1s^{-1}$ and $0.5s^{-1}$. The testing sheets of composites were

33   compression molded at 180 °C and 10 MPa into 17mm ×10mm ×1mm. The test was conducted

34   under nitrogen atmosphere.

35

36   **3. Results and discussion**

37

38   **3.1. Synthesis and characterization of MCC-g-PLA copolymers**
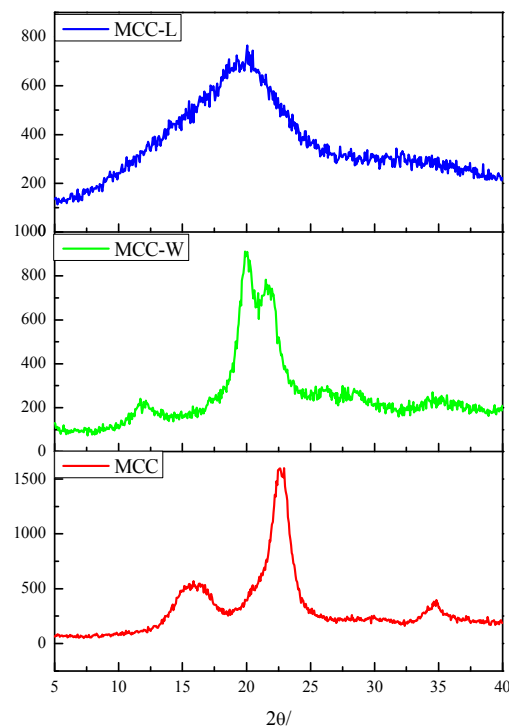
Figure 1. WAXD spectra of MCC, MCC-W and MCC-L

WAXD spectra of MCC, MCC-W and MCC-L were shown in Figure 1. Cellulose I and cellulose Ⅱ are the most commonly used cellulose, and in WAXD spectra cellulose I shows three characteristic diffraction peaks at around 2θ=14.8, 16.3 and 22.6°, whereas cellulose Ⅱ shows three peaks at around 2θ=12.1, 19.8 and 22.0° [43]. From Figure 1, MCC was a typical cellulose I, and MCC-W was a typical celluloseⅡ. But MCC-L was neither cellulose I nor cellulose Ⅱ, only a dispersive broad peak at 2θ=20.0° was observed.

In cellulose, the hydrogen-bonding network makes molecular chains arrange regularly and form crystal. Different from cellulose I with parallel chain structure, cellulose Ⅱ was comprised of an array of antiparallel chain molecules, and the unit cell was monoclinic according to Kolpak and Blackwell [44]. When MCC was treated in NaOH solution, alkali reached to amorphous and crystalline regions of MCC, and destroyed the hydrogen bonds in the crystalline regions, then MCC was dissolved in NaOH solution [47]. When dissolved MCC was regenerated in water, the conformation of hydroxymethyl group changed [43-45], and cellulose I transformed to cellulose Ⅱ with an antiparallel chain structure. So MCC-W was cellulose Ⅱ. But for cellulose Ⅱ, the hydrogen-bonding network and structure were also very dense, and the reaction reagents were still difficult to penetrate into the inside of cellulose and react with cellulose. So, simple alkali treatment could not improve the accessibility of cellulose. Therefore, if we wanted to introduce reaction reagents into cellulose, we had to use the stage when hydrogen bonds were destroyed.

According to the above analysis, after MCC was dissolved in NaOH solution, hydrogen bonds in cellulose were destroyed by alkali. At this time, if the reaction reagents were added into the mixture, reaction reagents may enter into the cellulose before the hydrogen bond regenerated. For MCC-L, perfect crystalline structure was not observed, indicating that the crystal structure and hydrogen-bonding network had been disrupted. This may be owing to that adding lactic acid into

1   the dissolved MCC solution did make lactic acid enter into cellulose, and the lactic acid remained

2   in cellulose after drying at 60 ^{o}C. The boiling point of lactic acid was about 122 ^{o}C [48], and it was

3   not easy to evaporate at 60 ^{o}C. This was also confirmed by increase in the weight of MCC-L

4   compared with MCC-W. The remained LA molecules formed steric hindrance to hinder the

5   configuration change of C-O bond at C6 position and the formation of hydrogen bonds, and broke

6   the regularity of hydrogen-bonding network in cellulose, thus MCC-L cannot crystallize. That is,

7   lactic acid had reached into the crystalline region of cellulose, and had a possibility of reacting

8   with hydroxyl groups both in amorphous and crystalline region, and the accessibility of cellulose

9   to lactic acid was improved.

10
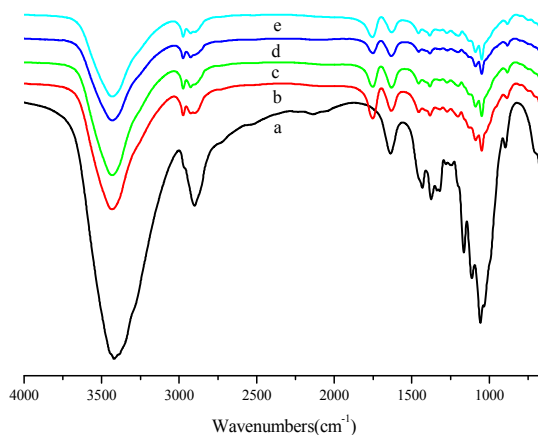
11

12   Figure 2. FTIR spectra of (a) MCC, (b) MP-C0W4-T130, (c) MP-C0W4-T140, (d)

13   MP-C0W4-T150, and (e) MP-C0W4-T160.

14   The structure of MCC-g-PLA copolymers was characterized by FTIR and the results were

15   presented in Figure 2. Because the byproduct PLA homopolymer produced in melt

16   copolycondensation process had been removed by purification process, the FTIR spectra should

17   reflect the chemical structure of the grafted copolymers. As shown in Figure 2, the strong peak at

18   around 3410cm^{-1} was assigned to the absorption of hydroxyl groups in cellulose. Compared with

19   FTIR result of MCC, a new band at about 1750cm^{-1} was observed in each grafted copolymer

20   spectrum, which was assigned to the carbonyl group. The methyl asymmetric deformation in PLA

21   side chains at around 1475cm^{-1}, and the symmetric C-O-C stretching modes in ester groups at

22   around 1200cm^{-1} also appeared in the spectra of the copolymers [49]. The results clearly proved that

23   PLA chains had been grafted onto cellulose backbone by melt copolycondensation of LA with

24   hydroxyl groups in cellulose and MCC-g-PLA copolymers were synthesized successfully, as

25   shown in Scheme 1.

26

27
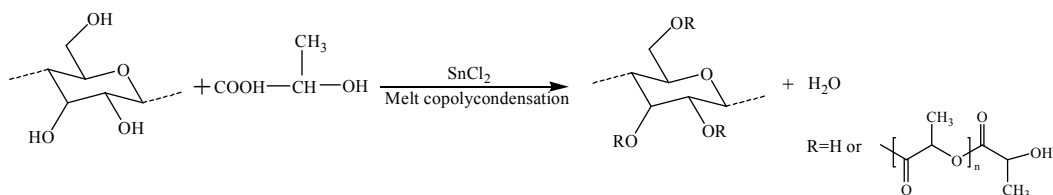
28

1   Scheme 1. Illustration of the melt copolycondensation of LA with MCC.

2   The structure of the copolymers was also investigated by ^{1}H NMR. An ^{1}H NMR spectrum

3   obtained for one MCC-g-PLA copolymer (MP-C0W4-T160) was displayed in Figure 3 and the

4   signal peaks were assigned as follows: δ=1.32 ppm (methyl protons of terminal lactyl); δ=1.50

5   ppm (methyl protons of internal lactyl); δ=4.23 ppm (methine protons of internal lactyl);

6   δ=5.07-5.29 ppm (methine protons of terminal lactyl); δ=3-5.4 ppm (protons of anhydroglucose).

7   The appearance of proton signals of lactyl groups in this spectrum, further confirmed that

8   MCC-g-PLA copolymers were synthesized successfully.

9   The contents of grafted PLA in cellulose-g-PLA copolymers were calculated according to [1]H

10   NMR spectra. As shown in Figure 3 , we designated the resonance peak area derived from methine

11   protons of internal lactyls in PLA side chains as A, and the resonance peak area from methine

12   protons of terminal lactyls as B. The resonance peak area derived from methyl protons of internal

13   lactyls was labeled as C, and the area from methyl protons of terminal lactyls was labeled as D.

14   The integral of all protons of anhydroglucose (AHG) unit was designated as E. Then the average

15   degree of polymerization of a PLA side chain (DP$_s$),   the degree of lactyl substitution (DS, the

16   average number of hydroxyl groups substituted for lactyls per AHG of cellulose), and the molar

17   substitution (MS, the average number of introduced lactyl units per AHG of cellulose) were

18   estimated by equations (1)-(3) [38, 40], respectively, and the results were summarized in Table 1.

19   $DP_s=(I_C+I_D)/I_D$ (1)

20   $DS=7I_D/3[I_E-(I_C+I_D)/3]$ (2)

21   $MS=DP_s\times DS$ (3)

22
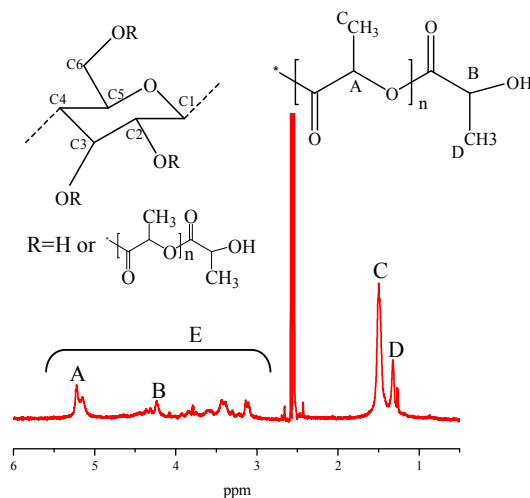
23

24   Figure 3. ^{1}H NMR spectrum of a MCC-g-PLA copolymer (MP-C0W4-T160)

25   According to Table1, the amount and length of PLA side chains can be controlled by adjusting

26   reaction conditions and molar ratios of LA monomer to MCC, and the relationship between them

27   will be discussed in detail subsequently.

28   From Table 1, the difference of the reaction conditions of samples MP-C0W4-TX (X=130, 140,

29   150, 160) was reaction temperature, where the average numbers of hydroxyl groups substituted for

30   lactyls per AHG (DS values) were almost constant, ranging from 0.60 to 0.67 with increasing

31   reaction temperature, meaning that the accessibility of LA monomer to cellulose kept the same.

1   Based on previous analysis, the accessibility of cellulose was mainly affected by solvent exchange
2   pretreatment process. So the influence of reaction temperature on DS was small. However DP_s
3   values of the four samples increased with the increasing of reaction temperature. Lactic acid
4   melting polycondensation reaction was an equilibrium reaction, producing PLA and water, so
5   removing water was beneficial to the conversion of lactic acid into PLA [50, 51]. Under the same
6   vacuum condition, high temperature could accelerate the removal of water, including free water
7   and that formed in reaction process. Besides, elevated temperature could also increase the thermal
8   degradation rate. Therefore, the influence of temperature on reaction was a combination of these
9   factors. In the temperature range of our experiments, the DP_s value increased with the temperature
10   rising.

11

12   Table 1. The reaction conditions, molar ratios of LA to AHG and ^{1}H NMR results of MCC-g-PLA
13   copolymers

Sample	Washing times	LA^a/AHG (mol/mol)	T(^{o}C)	DP_s	DS	MS
MP-C0W4-T130	4	0	130[b]	2.79	0.60	1.67
MP-C0W4-T140	4	0	140[c]	3.40	0.60	2.04
MP-C0W4-T150	4	0	150[d]	3.47	0.64	2.22
MP-C0W4-T160	4	0	160	4.67	0.67	3.13
MP-C1W4-T160	4	18/1	160	5.17	0.71	3.67
MP-C2W4-T160	4	36/1	160	4.60	0.64	2.94
MP-C2W3-T160	3	36/1	160	4.70	0.88	4.14
MP-C2W2-T160	2	36/1	160	5.90	0.88	5.19
MP-C2W1-T160	1	36/1	160	6.22	0.96	5.97

14   [a] indicates the amount added in melt copolycondensation process, which does not include the LA
15   remained in MCC-L;
16   [b] specific reaction temperature and time: 120 ^{o}C, 2h; 130 ^{o}C, 6h;
17   [c] specific reaction temperature and time: 120 ^{o}C, 2h; 130 ^{o}C, 2h; 140 ^{o}C, 4h;
18   [d] specific reaction temperature and time: 130 ^{o}C, 2h; 140 ^{o}C, 2h; 150 ^{o}C, 4h

19

20   Samples MP-CXW4-T160 (X=0, 1, 2) were synthesized by adjusting the molar ratios of LA
21   monomer to MCC. According to Table 1, with increasing molar ratios of LA/AHG, DS and DP_s
22   values of the copolymers showed no obvious changes, indicating that increasing the content of LA
23   monomer had almost no effect on the copolymers. Theoretically, increasing the content of reactant
24   was helpful to produce the product for an equilibrium reaction. But in our work, the melt
25   copolycondensation happened in a heterogeneous condition, and the steric hindrance influenced
26   the reaction, which made the added monomer not participate in the reaction completely, so the
27   influence of monomer content on graft copolymers was not so significant.
28   Except for the reaction process, the pretreatment process, in which we used solvent exchanged
29   method to change the accessibility of cellulose, also influenced the formation of copolymers.
30   The solvent exchanged process was related to the washing step with lactic acid in the pretreatment
31   process, then we wondered whether the washing times with lactic acid had influenced on the graft
32   copolymers. So we synthesized samples MP-C2WX-T160 (X=1,2,3,4) through the same reaction
33   process, only changing the washing times with lactic acid in pretreatment process.

1   From Table 1, we observed the dependence of DS and DP_s on washing times. Obviously, DS and
2   DP_s increased gradually when the number of washing times reduced, indicating that the
3   consumption of lactic acid can be reduced. During the process that the dissolved cellulose was
4   regenerated and washed with lactic acid, firstly, lactic acid entered into cellulose, and combined
5   with alkali, then the alkali was brought out of cellulose, at this time hydroxyl groups surrounded
6   by alkali were freed out. These free hydroxyl groups probably formed hydrogen bonds with other
7   free hydroxyl groups, or probably were surrounded by lactic acid again. If hydroxyl group
8   contacted with lactic acid, it had the possibility of reacting with LA. But, once it formed hydrogen
9   bond with other free hydrogen group, it was hard to take part in a reaction because the hydrogen
10   bonds were difficult to be broken again. So in each washing process, some hydroxyl groups which
11   were surrounded with alkali or lactic acid were freed out again and then formed hydrogen bonds,
12   thus losing the possibility of reaction. So with the increase of washing times, DS value decreased
13   gradually. The hydrogen bonds also limited the diffusion of lactic acid in cellulose, which affected
14   the amount of lactic acid that could participate in reaction, causing the decrease of DP_s.
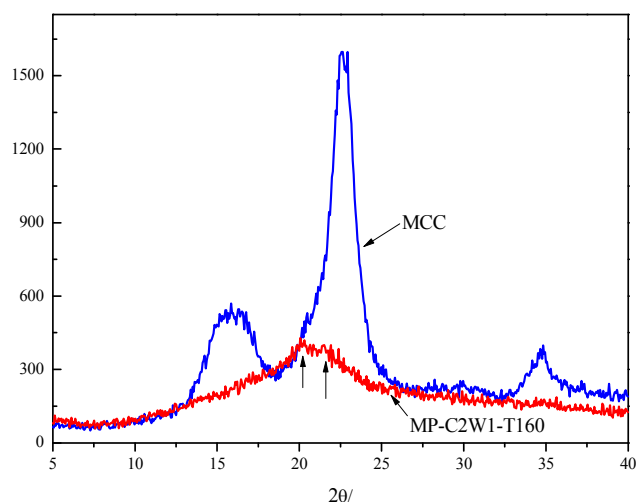
15

16   Figure 4. WAXD spectra of unmodified MCC and MP-C2W1-T160

17   The crystalline structures of MCC and MP-C2W1-T160 were studied by WAXD and the results
18   were shown in Figure 4 (Spectra of other copolymers were similar to MP-C2W1-T160 and not
19   shown here for brevity). MCC was a typical cellulose I, as mentioned above. Different from
20   WAXD spectrum of MCC, MP-C2W1-T160 showed two broad and small peaks at 19.8°and 22.0°,
21   which were the characteristic diffraction peaks of cellulose Ⅱ. The intensity of these two peaks
22   was very weak, and the characteristic peak at 12.1°did not appear, indicating that MCC-g-PLA
23   copolymers presented an imperfect crystalline structure of cellulose Ⅱ. According to Kolpak and
24   Blackwell [44], for cellulose Ⅱ intramolecular hydrogen bonds (O2'-H…O6) and intermolecular
25   hydrogen bonds (O6-H…O3, O6-H…O2) were in the 020 plane, and intermolecular hydrogen
26   bond (O2-H…O2') was in 110 plane. These hydrogen bonds made the molecular chains arrange
27   regularly and form a perfect crystal. Reaction between LA and hydroxyl group reduced the
28   amount of hydroxyl groups capable of forming hydrogen bonds. On the other hand, the existence
29   of PLA side chains generated steric hindrance, also affecting the formation of hydrogen bonds and

1 regular arrangement of molecular chains. So the hydrogen-bonding network was weakened and
2 MCC-g-PLA copolymers could not form perfect crystals. These result also proved that
3 copolycondensation reaction occurred both in amorphous and crystalline region. Therefore we had
4 improved the reactivity of cellulose by this method and synthesized MCC-g-PLA successfully.
5
6 **3.2. Thermal properties of MCC-g-PLA copolymers**
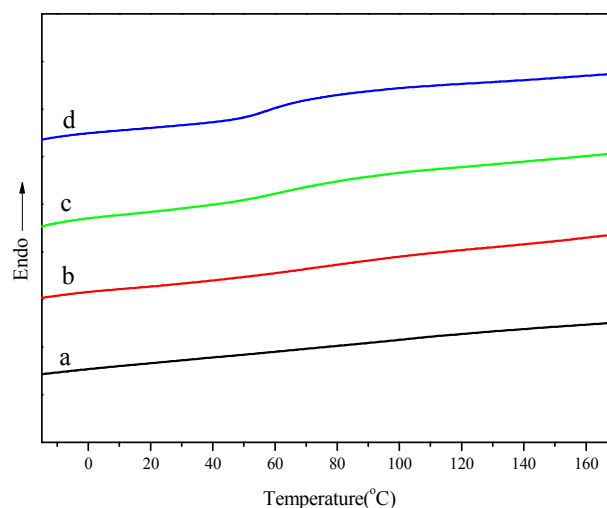
7
8 Figure 5. DSC curves of (a) MCC, (b) MP-C0W4-T130, (c) MP-C0W4-T160, and (d)
9 MP-C2W1-T160.
10 The thermal properties of MCC-g-PLA copolymers were investigated by DSC and TG
11 measurements. Figure 5 displayed the DSC curves of MCC and MCC-g-PLA copolymers
12 (MP-C0W4-T130, MP-C0W4-T160, MP-C2W1-T160) in the second heating scan, and T_g values
13 collected from second heating curves for all samples were listed in Table 2. From Figure 5, each
14 curve of MCC-g-PLA copolymers exhibited a baseline gap which reflected the glass transition
15 temperature T_g. However in the standard heating scan unmodified cellulose did not show a glass
16 transition temperature, Batzer and Kreibich [52] reported a T_g at about 230 ^{o}C for cellulose by using
17 a more sensitive method. It can be seen that Tg varied with the copolymer composition, T_g of
18 MP-C0W4-T130 was the highest, and T_g of MP-C2W1-T160 was the lowest. Compared to the
19 unmodified MCC, the remarkable decrease in T_g for MCC-g-PLA copolymers suggested that the
20 existence of PLA side chains broke the hydrogen-bonding network, expanded the intermolecular
21 distance, and improved the chain mobility. This was also confirmed by WAXD result. That is, the
22 grafted PLA side chains played an important role of internal plasticizer to the semi-rigid cellulose.
23
24 Table 2. Thermal properties of MCC, PLA and MCC-g-PLA copolymers

sample	DP_s	DS	MS	$T_g(^oC)$	$T_{onset}(^oC)$	$T_{max}(^oC)$
MP-C0W4-T130	2.79	0.60	1.67	77.50	248.1	317.8
MP-C0W4-T140	3.40	0.60	2.04	70.50	244.2	315.8
MP-C0W4-T150	3.47	0.64	2.22	70.50	253.7	312.9
MP-C0W4-T160	4.67	0.67	3.13	60.93	264.7	316.7

MP-C1W4-T160	5.17	0.71	3.67	58.56	257.7	321.5
MP-C2W4-T160	4.60	0.64	2.94	61.94	255.1	321.9
MP-C2W3-T160	4.70	0.88	4.14	62.79	242.3	285.7, 321.6
MP-C2W2-T160	5.90	0.88	5.19	59.99	239.4	277.1, 313.2
MP-C2W1-T160	6.22	0.96	5.97	57.42	216.4	256.7, 301.7
MCC					320.1	347.6

1
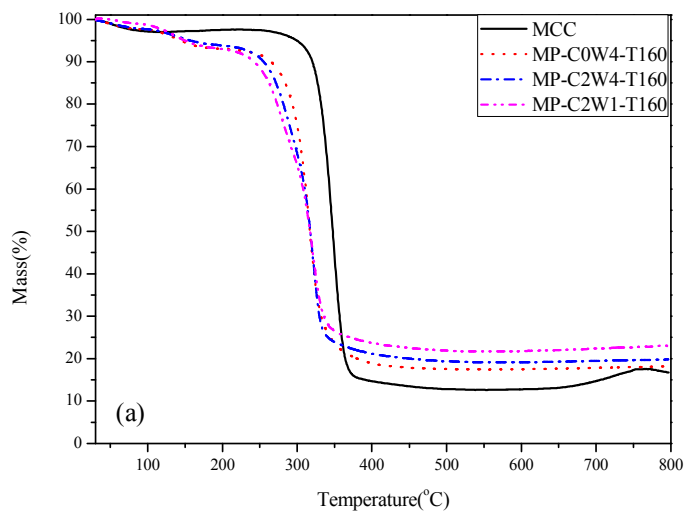
2
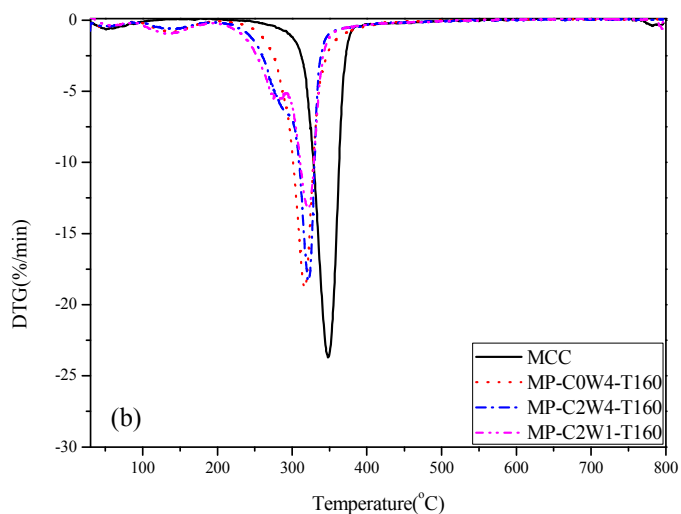
3

Figure 6. (a) TG and (b) DTG curves of MCC, MP-C0W4-T160, MP-C2W4-T160 and MP-C2W1-T160

TG measurement was used to evaluate the thermal stability of copolymers and the results were displayed in Figure 6 and Table 2. Obviously, the onset decomposition temperature (T_{onset}) and the maximum decomposition temperature (T_{max}) of MCC-g-PLA copolymers were lower than those of

1   MCC. It was owing to that the introduction of PLA side chains on the cellulose backbone
2   destroyed the hydrogen-bonding network and crystalline structure of MCC to some extent,
3   resulting in the decrease of thermal stability. This was also confirmed by DSC and WAXD results.
4   On the derivative thermogravimetry (DTG) curves, there was only one peak for copolymers when
5   MS<4.14, demonstrating that the thermal degradation of copolymers proceeded in one step.
6   Because the content of PLA side chains was low, the decomposition peak of PLA chains did not
7   emerge, and the peak in DTG curve was mainly caused by decomposition of cellulose backbone.
8   However a shoulder peak appeared near the main peak in DTC curves of MP-C1W4-T160 and
9   MP-C2W4-T160, showing that thermal decomposition process changed gradually. When
10 MS$\geq$4.14, two derivate thermogravimetry peaks appeared, indicating that thermal degradation of
11 these samples proceeded in two steps. This should be attributed to the different decomposition
12 temperatures of MCC backbone and PLA side chains, and the degradation occurring at low
13 temperature was caused by PLA side chains, and that at high temperature was caused by cellulose
14 backbone, which was also reported in literature [40].

15

16 **3.3. Structure and Properties of PLA/MCC-g-PLA composites**
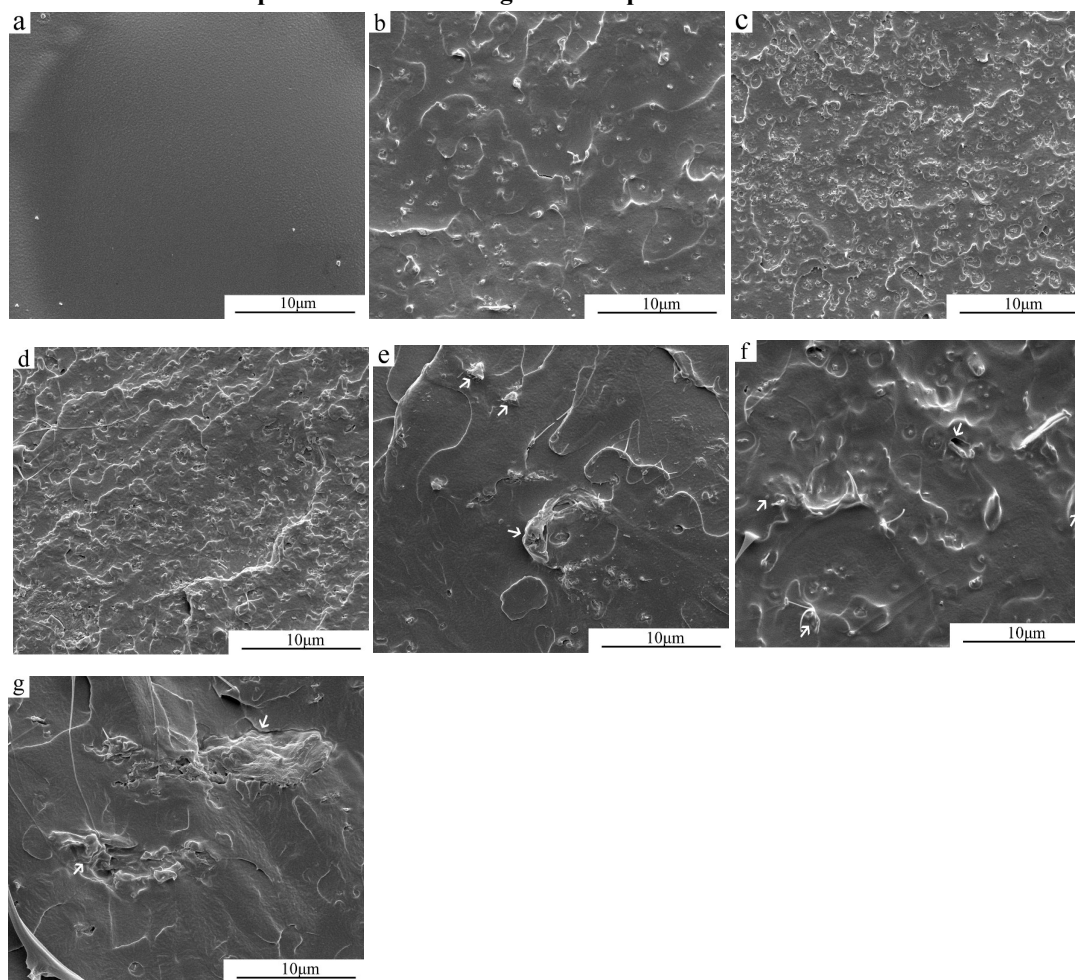
Figure 7. SEM micrograph of (a) PLA, (b) PLA-MP-2, (c) PLA-MP-3, (d) PLA-MP-4, (e) PLA-MCC-2, (f) PLA-MCC-3, and (g) PLA-MCC-4.

37 According to above analysis, PLA had been successfully grafted onto the MCC, and then sample

1   MP-C2W1-T160, which had the longest PLA side chains, was chosen and compounded into PLA

2   matrix to explore the influence of MCC-g-PLA copolymer on the structure and properties of PLA.

3   Improving the dispersion of cellulose in matrix is necessary to enhance the properties of such

4   composites [53], and the dispersion state of MCC-g-PLA in PLA matrix was revealed by SEM

5   micrograph shown in Figure 7. For neat PLA, the micrograph showed a smooth and flat fracture

6   surface. But it was changed to an uneven fracture surface with the addition of MCC-g-PLA, which

7   indicated that a signification PLA matrix deformation occurred. As is known, the compatibility of

8   PLA and cellulose was poor due to the hydrophobic nature of PLA and hydrophilic characteristic

9   of cellulose [38, 54]. So large-size aggregates of cellulose and void appeared in the fracture surfaces

10   of PLA/MCC composites, which was indicated with arrows in Figure 7 (e-g). However,

11   MCC-g-PLA dispersed well in the matrix, and there was no obvious large-size agglomeration,

12   showing that the existence of PLA side chains can greatly improve the dispersion state of

13   MCC-g-PLA in PLA matrix and inhibit the agglomeration of MCC-g-PLA and improve the

14   compatibility with PLA.
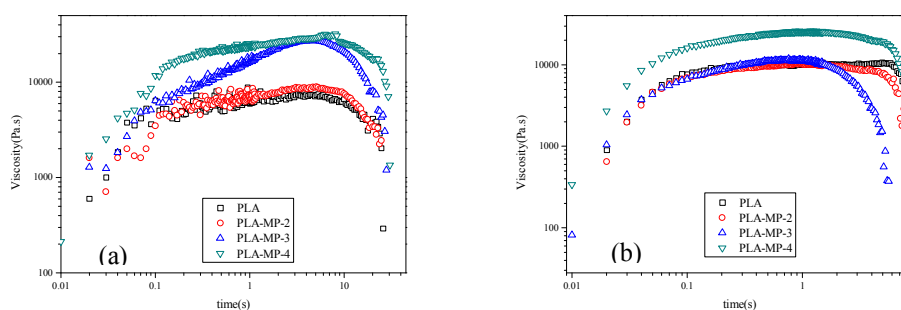
Figure 8. Variation of elongation viscosity as a function of time for PLA and PLA/MCC-g-PLA composites at 158.5 ^{o}C with elongation rates of (a) 0.1s^{-1} and (b) 0.5s^{-1}.

19   In order to investigate the influence of MCC-g-PLA on the melt strength of PLA, the extensional

20   rheological properties of PLA and PLA/MCC-g-PLA composites were characterized by the

21   extensional rheology at the extensional strain rates of 0.1s^{-1} and 0.5s^{-1} in steady uniaxial extension,

22   and the results were shown in Figure 8. It was obvious that the elongational viscosity of neat PLA

23   kept almost constant at the full time of stretching, and the strain-hardening behavior could not be

24   observed, which was the typical characteristic of linear polymer. The elongational viscosity was

25   improved with the addition of MCC-g-PLA at low extensional strain rate (0.1s^{-1}), and the

26   increment increased with increasing content of MCC-g-PLA, which was attributed to the

27   entanglement between MCC-g-PLA and PLA matrix. According to the ^{1}H NMR analysis of

28   MCC-g-PLA, the average degree of polymerization of PLA side chain was 6.22, that is the

29   average molecular weight was 425g/mol, however the critical molecular weight for entanglement

30   of PLA was near 9000g/mol [55], the length of PLA side chains in MCC-g-PLA was not long

31   enough to form strong entanglement with PLA matrix. So the entanglement should be between

32   MCC-g-PLA filler particles and PLA matrix, but not between the PLA side chain and PLA matrix.

33   However, at high extensional strain rate (0.5s^{-1}), when the content of filler was low (sample

34   PLA-MP-2 and PLA-MP-3), the elongational viscosity could not be improved and was

35   approximately equal to that of neat PLA; only PLA-MP-4 showed higher elongational viscosity

1   than neat PLA. According to the SEM results, MCC-g-PLA was well dispersed in the matrix, so

2   the higher the content of MCC-g-PLA, the more the entanglement in the composites. For

3   PLA-MP-2, due to the low entanglement, the elongational viscosity was almost equal to neat PLA

4   even at low extensional strain rate. For PLA-MP-3, the entanglement was increased, so the

5   elongational viscosity increased at low extensional strain rate. But at high extensional strain rate,

6   the elongational viscosity decreased because of disentanglement and was approximately equal to

7   neat PLA indicating hardly any entanglement between filler and matrix. For PLA-MP-4, the

8   elongational viscosity decreased with the increase of extensional strain rate, but was still higher

9   than neat PLA, showing that there was entanglement remained in spite of the existence of

10   disentanglement.
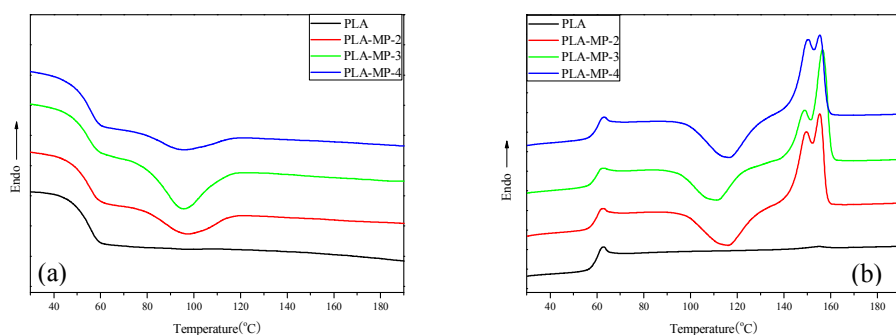
11

12   Figure 9. DSC thermograms of pure PLA and PLA/MCC-g-PLA composites (a) for the first

13   cooling process, (b) for the second heating process.

14   The effects of MCC-g-PLA on the non-isothermal crystallization and melting behaviors of PLA

15   matrix were also investigated by DSC. Cooling curves of different samples were shown in Figure

16   9(a). For pure PLA, there was no exothermic peak representing the crystallization of PLA in the

17   cooling curve due to the relatively rigid molecular chain and slow crystallization rate. However,

18   an exothermic peak emerged when MCC-g-PLA was introduced, and the peak became stronger

19   with increasing content of MCC-g-PLA, except for sample PLA-MP-4. In the second heating

20   process (Figure 9(b)), there was no cold crystallization peak, which was also observed in literature

21   [56, 57], and melting peak for pure PLA. For PLA/MCC-g-PLA composites, we observed the

22   appearance of cold crystallization peak, and the cold crystallization temperature (T_{CC}) shifted to

23   the lower temperature with increasing content of MCC-g-PLA, and returned to higher temperature

24   for PLA-MP-4. These results indicated that the addition of MCC-g-PLA acted as nucleation agent

25   and promoted the crystallization ability of PLA. At first, the nucleation ability of MCC-g-PLA was

26   enhanced with the increasing content of nucleation agent, thus making crystallization peak

27   become stronger and T_{CC} shift to lower temperature. Then the content of MCC-g-PLA increased

28   further, the entanglement between PLA and MCC-g-PLA also increased, resulting in the hindered

29   mobility of PLA molecular chains. This was in agreement with the extensional rheology test. In

30   addition, the shape of melting peak also changed with the content of MCC-g-PLA. As shown in

31   Figure 9 (b), there were double melting peaks in the second heating curves of PLA/MCC-g-PLA

32   composites, which was attributed to the melt/recrystallization behavior of PLA [58, 59]. The melting

33   peak at lower temperature was caused by the melting of imperfect crystals and the melting peak at

34   higher temperature was caused by the melting of the relatively perfect crystal and recrystallized

crystals. Taking PLA-MP-3 as an example, the crystallization ability was the strongest, and the amount of relatively perfect crystal formed in crystallization process was more, so the higher temperature melting peak was intensified.

4. Conclusions

A series of cellulose derivatives MCC-g-PLA copolymers with MS of PLA in a range of 1.67-5.97 were synthesized by melt copolycondensation of lactic acid with microcrystalline cellulose using $SnCl_2$ as catalyst. The factors of reaction temperature and washing times in pretreatment process had a great effect on the DS and DP_s value of graft copolymers. The resultant copolymers had an imperfect crystalline structure of cellulose Ⅱ due to the PLA side chains, which was comfirmed by WAXD measurements. All MCC-g-PLA copolymers exhibited a single T_g in second heating thermograms in DSC, and T_g varied from 77.50 ^{o}C to 57.77 ^{o}C in relation to the MS of PLA, indicating that the existence of PLA side chains had played an important role as internal plasticization. The thermal stability of MCC-g-PLA copolymer was lower than that of MCC, due to the weakened hydrogen-bonding network and crystallinity. When MS≥4.14, the thermal degradation of copolymers proceeded in two steps instead of one step, and the thermal decomposition behavior of PLA side chains appeared.
MCC-g-PLA copolymer can be well dispersed in PLA matrix, and the melt strength of PLA can be improved by the addition of MCC-g-PLA at low extensional strain rate, but the improvement decreased at high extensional strain rate, due to the weak entanglement. MCC-g-PLA also acted as nucleation agent to enhance the crystallization ability of PLA. The results in this work proved that the performance of PLA can be improved by this method, but the length of PLA side chains was short, if we improve its length over the critical entanglement length, the PLA side chain can also form entanglement with matrix, thus making melt strength increase significantly, so the studies on further improving the length of PLA side chains are now in progress.

Acknowledge

References

1 R. E. Drumright, P. R. Gruber and D. E. Henton, Adv. Mater., 2000, **12**, 1841-1846..

2 A. K. Mohanty, M. Misra and G. Hinrichsen, Macromol. Mater. Eng., 2000, **276-277**, 1-24.

3 M. Singhvi and D. Gokhale, *RSC Advances*, 2013, **3**, 13558-13568.

4 Y. Zhao, Z. Wang, J. Wang, H. Mai, B. Yan and F. Yang, J. Appl. Polym. Sci., 2004, **91**, 2143-2150.

5 T. Kaito, A. Myoui, K. Takaoka, N. Saito, M. Nishikawa, N. Tamai, H. Ohgushi and H. Yoshikawa, Biomaterials, 2005, **26**, 73-79.

6 H. S. Na and S. C. Kim, J. Macromol. Sci. A., 2010, **47**, 254-264.

7 F. Ge, Y. Ding, L. Yang, Y. Huang, L. Jiang and Y. Dan, RSC Adv., 2015, **5**, 70473-70481.

8 L. T. Lim, R. Auras and M. Rubino, Prog. Polym. Sci., 2008, **33**, 820-852.

9 D. Howard, K. Partridge, X. Yang, N. M. P. Clarke, Y. Okubo, K. Bessho, S. M. Howdle, K. M. Shakesheff and R. O. C. Oreffo, Biochem. Bioph. Res. Co. 2002, **299**, 208-215.

10 P. Zhang, Z. Hong, T. Yu, X. Chen and X. Jing, Biomaterials, 2009, **30**, 58-70.

11 H. Shi, Q. Gan, X. Liu, Y. Ma, J. Hu, Y. Yuan and C. Liu, RSC Adv., 2015, **5**, 79703-79714.

12 R. Auras, B. Harte and S. Selke, Macromol. Biosci., 2004, **4**, 835-864.

13 I. Kyrikou and D. Briassoulis, J. Polym. Environ., 2007, **15**, 125-150.

14 R. Bhardwaj and A. K. Mohanty, Biomacromolecules, 2007, **8**, 2476-2484.

15 H. Li and M. A. Huneault, Polymer, 2007, **48**, 6855-6866.

16 F. Wu, B. Zhang, W. Yang, Z. Liu and M. Yang, Polymer, 2014, **55**, 5760-5772.

17 M. Beaulne and E. Mitsoulis, J. Appl. Polym. Sci., 2007, **105**, 2098-2112.

18 X. Lan, X. Li, Z. Liu, Z. He, W. Yang and M. Yang, J. Macromol. Sci. A., 2013, **50**, 861-870.

19 Y. Di, S. Iannace, E. Di Maio and L. Nicolais, Macromol. Mater. Eng., 2005, **290**, 1083-1090.

20 R. Mehta, V. Kumar, H. Bhunia and S. N. Upadhyay, J. Macromol. Sci. C., 2005, **45**, 325-349.

21 H. J. Lehermeier and J. R. Dorgan, Polym. Eng. Sci., 2001, **41**, 2172-2184..

22 L. Wang, X. Jing, H. Cheng, X. Hu, L. Yang and Y. Huang, Ind. Eng. Chem. Res., 2012, **51**, 10088-10099.

23 D. Auhl, J. Stange, H. Münstedt, B. Krause, D. Voigt, A. Lederer, U. Lappan and K. Lunkwitz, Macromolecules, 2004, **37**, 9465-9472.

24 D. Roy, M. Semsarilar, J. T. Guthrie and S. Perrier, Chem. Soc. Rev., 2009, **38**, 2046-2064.

25 S. J. Eichhorn, A. Dufresne, M. Aranguren, N. E. Marcovich, J. R. Capadona, S. J. Rowan, C. Weder, W. Thielemans, M. Roman, S. Renneckar, W. Gindl, S. Veigel, J. Keckes, H. Yano, K. Abe, M. Nogi, A. N. Nakagaito, A. Mangalam, J. Simonsen, A. S. Benight, A. Bismarck, L. A. Berglund and T. Peijs, J. Mater. Sci., 2010, **45**, 1-33.

26 H. Lönnberg, Q. Zhou, H. Brumer, T. T. Teeri, E. Malmström and A. Hult, Biomacromolecules, 2006, **7**, 2178-2185.

27 W. Yuan, J. Yuan, F. Zhang and X. Xie, Biomacromolecules, 2007, **8**, 1101-1108.

28 M. Krouit, J. Bras and M. N. Belgacem, Eur. Polym. J., 2008, **44**, 4074-4081.

29 Y. Teramoto and Y. Nishio, Polymer, 2003, **44**, 2701-2709.

30 X. Samain, V. Langlois, E. Renard and G. Lorang, J. Appl. Polym. Sci., 2011, **121**, 1183-1192.

31 X. Zhang, J. Zhao, L. Cheng, C. Lu, Y. Wang, X. He and W. Zhang, RSC Adv., 2014, **4**, 55195-55201.

32 A. Jayalakshmi, I.-C. Kim and Y.-N. Kwon, RSC Adv., 2015, **5**, 48290-48300.

33 M. Ioelovich, BioResources, 2009, **4**, 1168-1177.

34 C. L. McCormick, P. A. Callais and B. H. Hutchinson, Macromolecules, 1985, **18**, 2394-2401.

35 T. Röder, B. Morgenstern, N. Schelosky and O. Glatter, Polymer, 2001, **42**, 6765-6773.

36 H. Zhang, J. Wu, J. Zhang and J. He, Macromolecules, 2005, **38**, 8272-8277.

37 A. Mayumi, T. Kitaoka and H. Wariishi, J. Appl. Polym. Sci., 2006, **102**, 4358-4364.

38 H. Dong, Q. Xu, Y. Li, S. Mo, S. Cai and L. Liu, Colloid. Surface. B., 2008, **66**, 26-33.

39 S. Xiao, T. Yuan, H. Cao, D. Lin, Y. Shen, J. He and B. Wang, BioResources, 2012, **7**, 1748-1759.

40 C. Yan, J. Zhang, Y. Lv, J. Yu, J. Wu, J. Zhang and J. He, Biomacromolecules, 2009, **10**, 2013-2018.

41 L. Dai, D. Li and J. He, J. Appl. Polym. Sci., 2013, **130**, 2257-2264.

42 Y. Zhang, X. Li, Y. Yang, A. Lan, X. He and M. Yu, RSC Adv., 2014, **4**, 34584-34590.

43 A. Isogai, M. Usuda, T. Kato, T. Uryu and R. H. Atalla, Macromolecules, 1989, **22**, 3168-3172.

44 F. J. Kolpak and J. Blackwell, Macromolecules, 1976, **9**, 273-278.

RSC Advances Accepted Manuscript

45 P. Langan, Y. Nishiyama and H. Chanzy, Biomacromolecules, 2001, **2**, 410-416.

46 P. K. Gupta, V. Uniyal and S. Naithani, Carbohydr. Polym., 2013, **94**, 843-849.

47 A. Isogai and R. H. Atalla, Cellulose, 1998, **5**, 309-319.

48 M. G. Porter and R. S. Murray, Grass Forage Sci., 2001, **56**, 405-411.

49 Y. Luan, J. Wu, M. Zhan, J. Zhang, J. Zhang and J. He, Cellulose, 2013, **20**, 327-337.

50 E. M. Filachione and C. H. Fisher, Ind. Eng. Chem., 1944, **36**, 223-228.

51 S. I. Moon, C. W. Lee, M. Miyamoto and Y. Kimura, J. Polym. Sci. Pol. Chem., 2000, **38**, 1673-1679.

52 H. Batzer and U. Kreibich, Polym. Bull., 1981, **5**, 585-590.

53 B. Braun and J. R. Dorgan, Biomacromolecules, 2009, **10**, 334-341.

54 E. Espino-Pérez, J. Bras, V. Ducruet, A. Guinault, A. Dufresne and S. Domenek, Eur. Polym. J., 2013, **49**, 3144-3154.

55 J. R. Dorgan, J. Janzen, M. P. Clayton, S. B. Hait and D. M. Knauss, J. Rheol., 2005, **49**, 607-619.

56 J. M. Raquez, Y. Murena, A. L. Goffin, Y. Habibi, B. Ruelle, F. DeBuyl and P. Dubois, Compos. Sci. Technol., 2012, **72**, 544-549.

57 E. Fortunati, I. Armentano, Q. Zhou, D. Puglia, A. Terenzi, L. A. Berglund and J. M. Kenny, Polym. Degrad. Stabil., 2012, **97**, 2027-2036.

58 T. Dobreva, J. M. Pereña, E. Pérez, R. Benavente and M. García, Polym. Composite., 2010, **31**, 974-984.

59 Y. Song, K. Tashiro, D. Xu, J. Liu and Y. Bin, Polymer, 2013, **54**, 3417-3425.
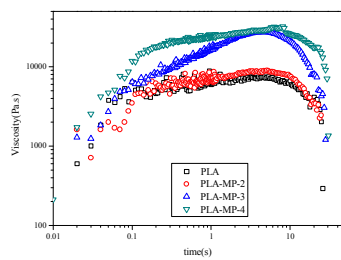
MCC-g-PLA copolymer can improve the elongational viscosity of PLA at elongation rates of $0.1s^{-1}$